Detection of Atherosclerotic Plaque Composition Using Intravascular Images

A. Taki MSc[1], M. Maadani MD[2], S. Setarehdan PhD[1], A. Roodaki M.SC[1], H. R. Sanati MD[2] and N. Navab PhD[3]

Abstract

Acute coronary syndromes (ACS) and sudden cardiac death are the main causes of morbidity and mortality in the world.[1] ACS are often the first manifestation of coronary artery disease, and the rupture of a coronary plaque is the main cause of ACS. Histopathological studies have revealed that the majority of thrombi result from plaque rupture.

Grayscale intravascular ultrasonography (IVUS), a tomographic imaging tool, can visualize coronary atherosclerosis *in vivo*, elucidating plaque area, plaque distribution, lesion length, and coronary remodeling. IVUS has demonstrated the discrepancies between the extent of atherosclerosis seen by coronary angiography and the actual extent of atherosclerotic disease.[2] Quantitative assessment of plaque composition has, however, not been possible with grayscale IVUS analysis, until now[3] ***(Iranian Heart Journal 2009; 10 (3):36-43).***

Key words: atherosclerosis■ plaque■ intravascular ultrasound

Post-mortem analyses have shown that thin-cap fibroatheroma (TCFA) is probably the main precursor lesion for plaque rupture.[4] TCFAs are characterized by a large necrotic core separated from the coronary lumen by a thin fibrous cap.

IVUS enables real-time, high-resolution tomographic visualization of the coronary arteries. Both lumen and vessel dimensions and the distribution of plaques can be analyzed. In addition, grayscale IVUS can be used to assess the presence of intraluminal thrombus and plaque rupture. [5]

Grayscale IVUS has demonstrated the multiplicity of plaque ruptures seen in patients with ACS.[6-8] A recent study showed that the number of vulnerable plaques with less than 75% luminal obstruction identified by IVUS had a positive correlation with future cardiovascular events. [9]

Grayscale IVUS imaging is, however, limited with regards to the analysis of plaque composition. Both calcified and dense fibrotic tissues such as those found in plaques have strong echo-reflections with lateral shadowing and are, therefore, not easy to differentiate. As a consequence, the extent of calcification is often overestimated. Areas with low echo-reflections comprise foam cells or necrotic core, fibrotic tissue, intraplaque hemorrhage, and fresh or still-organizing intraluminal thrombus. Currently, VH-IVUS can better distinguish between areas with low echo-reflections than can grayscale IVUS. Nevertheless, quantification of hypo-echogenicity is promising, as it has been related to an adverse event rate. [10,11]

The tedious and time-consuming task of manual processing and interpretation of images suffers from intra- and interobserver

Received May 22, 2008; Accepted for publication Oct . 24, 2009
From the (1)Control and Intelligence Processing Center of Excellence , Faculty of Electrics and Computer Engineering, University of Tehran, Iran, (2)Shaheed Rajaie Cardiovascular Medical and Research Center , Tehran , Iran, and (3)Department of Computer Aided Medical Procedures (CAMP)- TU Munich, Germany
Correspondence to : M. Maadani, MD, Assistant Professor in Cardiology, Shaheed Rajaie Cardiovascular Medical and Research Center, Vali-Asr Ave, Mellat Park, Tehran, Iran.
Tel: +982-23922133 Email : mohsenmaadani@hotmail.com

variability. Furthermore, an expert may not be able to completely characterize the different composition of atherosclerotic plaques. Thus automatic characterization of IVUS images is inevitable.

Recently, several methods have been proposed for characterizing atherosclerosis composition using the IVUS technique.[12-17] Generally, there are two ways of analyzing the IVUS data: the first one is to examine the IVUS images by extracting efficient textural features from every image and assign each pixel to one of the predefined classes.[12,13] The drawback of this method is that during the construction of each image from its corresponding signals, some important information, which may differentiate various tissues types efficiently, could be disregarded.

The second approach is to study IVUS backscattered signals, and a novel method based on the processing of signal power spectrum has been proposed.[14-17] This method is known as "Virtual Histology" (VH).

The results of the *in vivo* IVUS RF data analysis, i.e. IVUS-VH, are reported to be highly correlated with those of histopathology.[18,19] Many investigations have demonstrated the efficacy of this method for the classification of the different types of coronary plaque components.

Nowadays, VH is a widely accepted imaging modality and is being extensively used in many clinical approaches.[18-21] Perhaps the only limitation of this technique is the large storage needed for saving the IVUS backscattered signal of every subject.

As outlined previously, many different cell and tissue types are commonly found in atherosclerotic plaques. To simplify image interpretation and because of the fundamental resolution limitations of the underlying ultrasound signal, plaque components are grouped into four basic tissue types during VH-IVUS imaging. These components are displayed on VH-IVUS as different color pixels (Fig. 1).

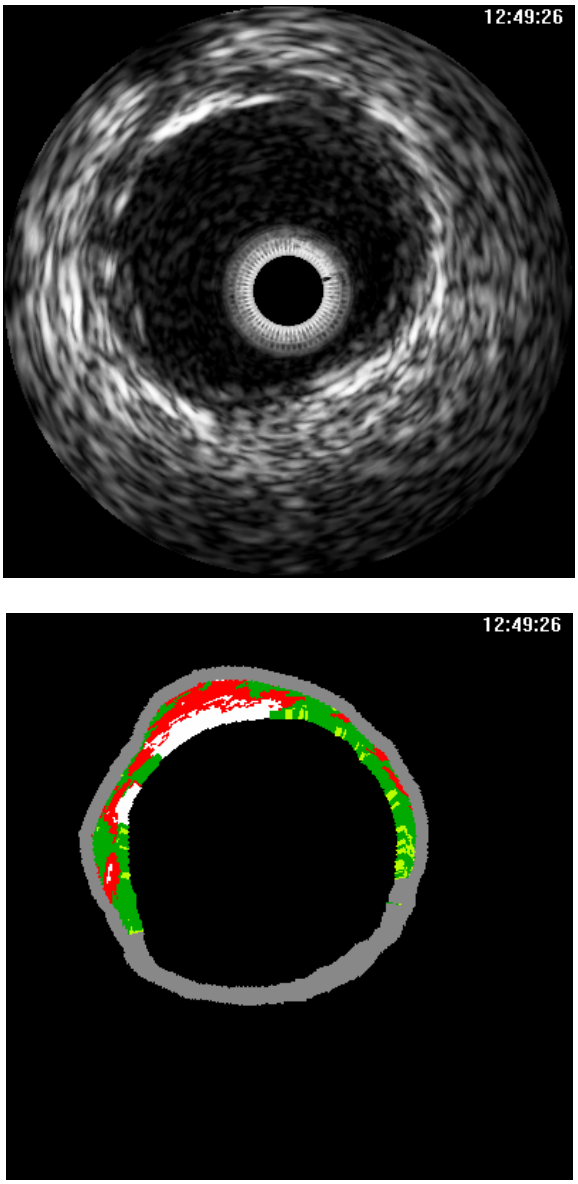

Fig. 1. An IVUS image sample above with its corresponding IVUS-VH below

Fibrous tissue is represented as dark green pixels. Histologically, this tissue type is characterized by bundles of collagen fibers with little to no lipid accumulation in or around the fibrous area. On grayscale IVUS, this tissue tends to be bright to medium-bright regions and generally has no acoustic shadow behind. Fibro-fatty tissue is denoted in VH-IVUS by light green pixels. This tissue is characterized by loosely packed collagen fibers (fibrous tissue) and proteoglycans, and

can be cellular, with or without interspersed foam cells. Extracellular matrix is abundant in this tissue type; moreover, there is no necrotic core and cholesterol clefts are very rare. Macrophages are also sometimes present, indicating an initial or ongoing inflammatory response. Groups of light green fibrofatty pixels on VH-IVUS are sometimes referred to as a 'lipid pool', which were thought, albeit inappropriately, to be rupture-prone. Lipid pools were initially thought to represent a loss of the tissue matrix that is rich in lipids but does not represent a necrotic core. As such, in fibrofatty areas there is no 'necrotic core' to rupture. At an advanced stage, the accumulation of fibrofatty tissue is referred to as pathologic intimal thickening.

In VH-IVUS, the necrotic core is represented by red pixels. In histology, this tissue type is characterized by a high concentration of extracellular lipid within a necrotic core that is made up of remnants of dead, lipid-filled smooth muscle cells, foam cells, trapped red blood cells, and fibrin. Little to no collagen is present and a matrix-like cellular structure is absent. The loss of tissue matrix means that these 'necrotic cores' are rich in lipid, consisting predominantly of cholesterol monohydrate, cholesterol ester, and phospholipids. This tissue, therefore, has poor mechanical stability. Microcalcification, areas of solid calcification, and calcification of collagenous tissue are often observed as a by-product of the dead and dying cells. On grayscale IVUS, these microcalcifications tend to reflect the ultrasound signal more strongly than other components, and as a result areas of necrotic core can appear moderately bright white, with or without shadow.

White pixels represent dense calcium on VH-IVUS. This tissue is characterized by compact calcium crystals, as seen on histological specimens. On grayscale IVUS, these areas tend to act as extremely strong reflectors of the ultrasound signal, and appear as bright white with dark shadow behind. As with densely packed fibrosis, 'speckled' grains of calcium are bright white on grayscale, but have little or no shadow. This imaging pattern occurs when the spaces between the 'grains' of calcium are separated by other tissue types allowing the passing of the ultrasound signal without significant attenuation.

In this paper, we propose a technique for characterizing coronary plaque compositions via processing IVUS images. First, the image is transformed into polar coordinates, and then textural features are extracted from the polarized images. These features are thereafter classified using a multilayer perceptron (MLP) artificial neural network.

In the feature extraction section, two well-known feature extraction techniques, co-occurrence[22] and local binary pattern (LBP),[23] are employed. The constructed IVUS-VH images are subsequently used for validating these two techniques.

There are four classes in IVUS-VH images: calcium, fibrous, fibrolipidic, and necrotic core. Areas exhibiting mild to heavy lipid accumulation are diagnosed as fibrolipidic. Thus, the fibrolipidic areas exhibit a large variation in intensity levels, making it hard to classify all four plaque types at just one step. Therefore, we combine the fibrous and fibrolipidic classes. Consequently, the region between intima and media-adventitia borders, which is known to be where the plaques exist, is classified into three classes. To ensure the compatibility of the results and validity of the comparisons, the same borders detected in the VH images were used in this study.

Methods

IVUS image processing methods provide measures of plaque composition without having to deal with a large amount of data points within the RF signals. This requires the useful and specific features to be extracted from the pixels belonging to the plaque regions within the images first. Different feature extraction and texture analysis methods have been used for this purpose, but

none has found widespread use in medical applications.[12]

The Co-occurrence Algorithm

A second-order statistical approach in which textural features are derived from angular nearest-neighbor spatial-dependence matrices known as co-occurrence matrices has been proposed. [20] Images were first quantized to 64 gray levels (Ng=64); a 64-level quantization was empirically chosen to maximize the algorithm efficiency and overall classification performance. The co-occurrence matrix was then formed by generating a two-dimensional matrix of size Ng × Ng. Given a quantized input image or region of interest, the co-occurrence value P (i, j, d, θ) represents the number of times two gray levels, i and j, occur at a given distance, d, and orientation, θ, from each other. A distance of one pixel was chosen because the regions of interest were small. All four possible orientations (0°, 45°, 90°, 135˚) can be averaged to ensure rotational invariance. From the co-occurrence matrix, 14 statistical features were computed. Each feature measured a particular characteristic of the spatial distribution relationship between neighboring pixels in the region of interest.

The Local Binary Pattern Algorithm

Local Binary Patterns (LBP) are structure related measures.[23] The operator detects "uniform" local binary patterns within circularly symmetric neighborhoods of P members on a circle of radius R and is given by $LBP_{R,P}^{riu2}$. Some neighbor sets are shown in Figure 2. In addition to $LBP_{R,P}^{riu2}$, which is rotation and gray-scale invariant, the $VAR_{P,R}$, which considers the variation of gray-scales in that region, and also the decimal representation of the binary sequence are extracted from every circle.

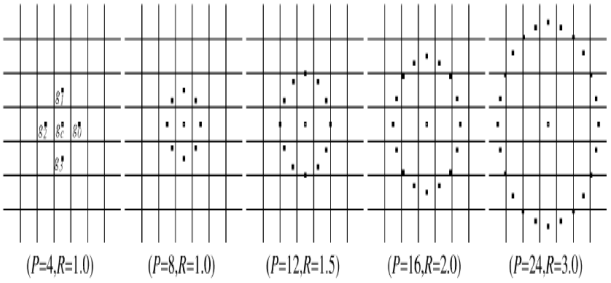

Fig. 2. Circularly symmetric neighbor sets for different (P, R)

Results

Our study group consisted of sequences of IVUS images acquired from five patients. These images with the digitized matrix size of 400x400 pixels were acquired using a 30-MHz transducer at a 0.5 mm/s pullback speed. Out of the frames in which all types of plaques were detected by the VH method, 20 frames were selected for each patient. The three mentioned methods were then applied to the set of 100 frames. The characterized IVUS images were validated by their corresponding VH images; and the accuracy, sensitivity, and specificity parameters were calculated for each technique. The results for each method were compared to each other.

The size of sweeping windows was empirically chosen to be 7x7. This was done the get the optimum results for every method separately. By assigning the size of window for LBP method to 7x7, two circles were constructed in each window.

Three features were thereafter extracted from each circle; the number of features for every pixel in LBP method thus summed up to nine. Extracting features from three circles with different radii can be thought of as a multi-resolution textural analysis.

The images were decimated to 64 gray-levels in co-occurrence. This was done to make the algorithm computationally more efficient.

This decimation did not affect the comparison between these three methods, as LBP is a gray-level invariant method.

The leave-one-patient cross-validation method was used to evaluate the performance of the algorithms; for every patient of the data set, the other four patients' images were used for training and the selected images were used for testing the MLP. The results are then averaged over all patients.

The number of neurons of each layer of the three-layer MLP was empirically chosen to be 21-3-3 and 10-3-3 for co-occurrence and LBP, respectively. The differences in the number of hidden neurons were caused by the differences in the dimension of feature vectors in each method. The comparative results of our proposed method and those of others are illustrated in the Table I.

Table I. The results of proposed methods

	Calcium		Fibrolipid		Necrotic		Overall
	Sensitivity	Specificity	Sensitivity	Specificity	Sensitivity	Specificity	
LBP	66%	92%	87%	77%	41%	88%	75%
Co-occurrence	70%	93%	91%	77%	43%	89%	79%

It can be inferred from Table I that the co-occurrence method has more capability for classifying all plaque types in comparison with the LBP method. However, the time efficiency of LBP method was much more desirable than that of the co-occurrence method. Figure 3 shows the performance of these two feature extraction methods in comparison with the corresponding constructed IVUS-VH image.

Discussion

Compared with other diagnostic tools, VH-IVUS provides improved *in vivo* diagnostic accuracy of atherosclerotic plaques.

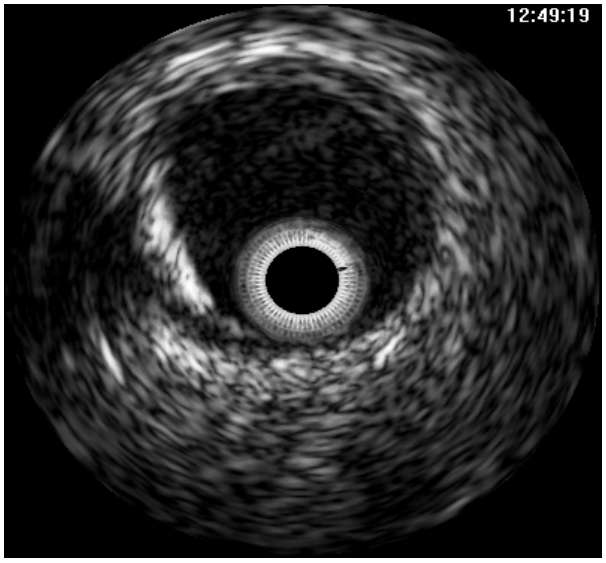

A

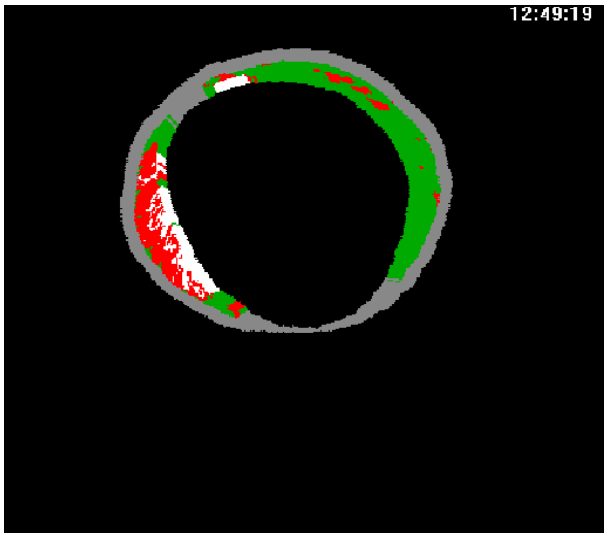

B

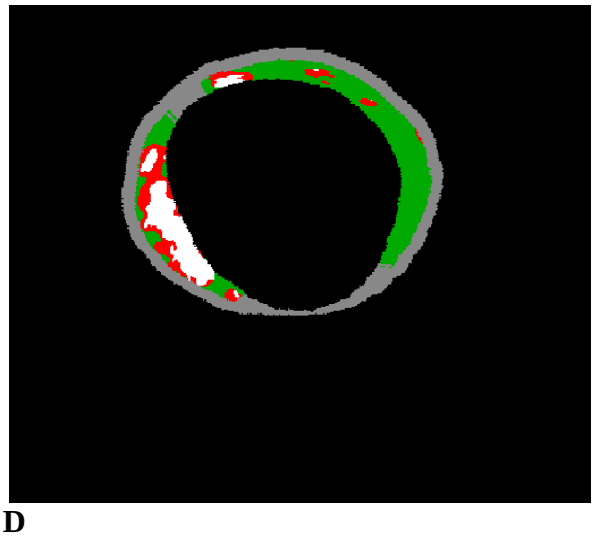

D

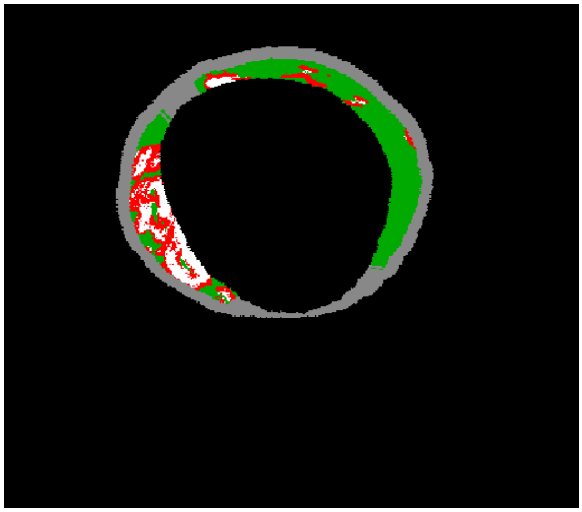

C

Fig. 3. (a) IVUS sample image, (b) corresponding three-class IVUS-VH, (c) characterized image using the co-occurrence method, and (d) LBP method

Of all currently available diagnostic tools, the pathology-based criteria for plaque vulnerability regarding plaque composition and plaque type can be most comprehensively assessed by grayscale IVUS and VH-IVUS. This evaluation enables a more comprehensive risk assessment and stratification on an individual basis for secondary prevention.

VH-IVUS guidance of coronary interventions may achieve complete coverage of virtual histologically defined high-risk lesions, in addition to the treatment of minimum lumen area, and therefore reduce the risk of restenosis or progression of atherosclerosis in the reference segments. The efficacy of this application, in comparison with that of optimum medical therapy, is also yet to be determined.

Until now, we have had no diagnostic tools and no evidence to support the treatment of vulnerable lesions with a preventive strategy other than risk factor modification. There is uncertainty regarding the restenosis risk after preventative stent treatment of vulnerable lesions in comparison with the spontaneous rupture rate of high-risk lesions that have not been treated with stenting. The duration of possible vulnerable stage is also unknown, as is the time of the progression or regression of coronary artery disease. Given that the vulnerability of high-risk lesions could be only temporary owing to the possibility of changes in plaque structure, prospective, serial VH-IVUS studies should be performed to clarify the natural history of these vulnerable lesions.

Our knowledge of the natural history of atherosclerosis, including lesion classification, relies on post-mortem histology data. As VH-IVUS enables *in vivo* identification of four different plaque characteristics and their location, this technique may confer a more accurate classification of lesions with regard to progression and regression. With time, we may even be able to determine with high accuracy which lesions should be treated with intervention and which with systemic medical therapy.

Conclusion

In this paper, the ability of the two feature extraction methods for the characterization of arthrosclerosis plaque compositions was investigated. The results of this study show that co-occurrence seems to be more powerful than the LBP method in term of classification accuracy.

One of the limitations of the co-occurrence technique is the high computational complexity of its features. By decimating the images to 64 grayscale, we managed to expedite this method. The drawback of the gray level decimation is, however, that there is a potential loss of information. Be that as it may, the human expert seems to pay more attention to the qualitative differences of intensities when characterizing IVUS images.

In general, there are some differences between the image processing and signal processing techniques. Obviously, in signal processing methods, the frequency information of RF signal is used along with

its amplitude, whereas in image processing techniques, decisions are made from the variations in the distribution of gray levels produced solely from the amplitude information of the RF signal. Hence, there is a possible loss of information in image processing techniques. Moreover, transformations into polar space and back into Cartesian coordinates is not error-free.

In this study, an IVUS image processing technique was evaluated with a signal processing one. Since both of these techniques have their pitfalls and are not perfect, where possible, it would be much more plausible to judge the proposed method against a ground truth obtained by histology.

As was mentioned earlier, the number of classes was reduced to three classes instead of four, by combining the fibrous and fibrolipid classes. The next challenge is to further classify the fibrous and fibrolipid areas.

References

1. Yusuf S, Reddy S, Ôunpuu S, Anand S. Global burden of cardiovascular diseases: part II - variations in cardiovascular disease by specific ethnic groups and geographic regions and prevention strategies. Circulation 2001; 104: 2855-2864.

2. Nissen SE, Yock P: Intravascular ultrasound: novel pathophysiological insights and current clinical applications. Circulation 2002; 103: 604-616.

3. Nissen SE: Application of intravascular ultrasound to characterize coronary artery disease and assess the progression or regression of atherosclerosis. Am J Cardiol 2002; 89: 24B-31B.

4. Virmani R. Pathophysiology of the vulnerable plaque. J Am Coll Cardiol 2006; 47 (8): (Suppl): C13-C18.

5. Potkin BN, Bartorelli AL, Gessert JM, Neville RF, Alma- gor Y, Roberts WC, Leon MB. Coronary artery imaging with intravascular high-frequency ultrasound. Circulation 1990; 81: 1575-1585.

6. Tanaka A, Shimada K, Sano T, Namba M, Sakamoto T, Nishida Y, Kawarabayashi T, Fukuda D, and Yoshikawa J. Multiple plaque rupture and C-reactive protein in acute myocardial infarction. J Am Coll Cardiol 2005; 45: 1594-1599.

7. Rioufol G, Rioufol G, Finet G, Ginon I, André-Fouët X, Rossi R, Vialle E, Desjoyaux E, Convert G, Huret JF, Tabib A. Multiple atherosclerotic plaques rupture in acute coronary syndrome: a three-vessel intravascular ultrasound study. Circulation 2002; 106: 804-808.

8. Schoenhagen P, Stone GW, Nissen SE, Grines CL, John G, Clemson BS, Vince DG, Ziada K, Crowe T, Apperson-Hanson C, Kapadia SR ; and Murat Tuzcu EM. Coronary plaque morphology and frequency of ulceration distant from culprit lesions in patients with unstable and stable presentation. Arterioscler Thromb Vasc Biol 2003; 23: 1895-1990.

9. Yamagishi M, Terashima M, Awano K, Kijima M, Nakatani S, Daikoku S, Ito K, Yasumura Y, and Miyatake K. Morphology of vulnerable plaque: insights from follow-up patients examined by intravascular ultrasound before an acute coronary syndrome. J Am Coll Cardiol 2002; 35: 106-111.

10. Mathiesen EB, Bønaa KH Joakimsen O. Ultrasonic echo-lucent carotid plaques are associated with high risk of ischemic cerebrovascular events in carotid stenosis: the Tromso study. Circulation 2001; 103: 2171-2175.

11. Grønholdt MLM, Nordestgaard BG, Schroeder TV, Vorstrup S, Sillesen H. Ultrasonic echolucent carotid plaques predict future strokes. Circulation 2002; 104: 68-73.

12. Vince DG, Dixon KJ, Cothren RM, Cornhill JF. Comparison of texture analysis methods for the characterization of coronary plaques in intravascular ultrasound images. Computerized Medical Imaging and Graphics, Vol. 24, pp. 221–229, 2000.

13. Caballero KL, Barajas J, Pujol O, Salvatella N, Radeva P. In-Vvivo IVUS tissue classification: a comparison between RF signal analysis and reconstructed images. 11th Iberoamerican Congress on Pattern Recognition (CIARP06),

LNCS 4225: 137-146, Cancun (Mexico) 11—2006.

14. Nair A, Kuban BD, Tuzcu EM, Schoenhagen P, Nissen SE, Vince DG. Coronary plaque classification using intravascular ultrasound radiofrequency data analysis. Circulation 2002; 106; 2200-2206.

15. Nair A, Calvetti D, Vince DG. Regularized autoregressive analysis of intravascular ultrasound backscatter: Improvement in spatial accuracy of tissue maps. IEEE Transactions on Ultrasonics Ferroelectrics and Frequency Control, vol. 51, pp. 420-431, 2004.

16. Nair A, Margolis MP, Kuban BD, Vince DG. Automated coronoary plaque characterisation with IVUS backscatter-ex vivo validation. EuroIntervention 2007.

17. Murashige A, Hiro T, Fujii T, Imoto K, Murata T, Fukumoto Y, Matsuzaki M. Detection of lipid laden atherosclerotic plaque by wavelet analysis of radiofrequency intravascular ultrasound signals. Journal of the American College of Cardiology 2005; 45: 12.

18. Rodriguez-Granillo GA, McFadden EP, Valgimigli M. Coronary plaque composition of nonculprit lesions, assessed by *in vivo* intracoronary ultrasound radiofrequency data analysis, is related to clinical presentation. American Heart Journal 2006; 151: 5.

19. Nasu K, Tsuchikane E, Katoh O, Vince DG, Virmani R. Accuracy of *in vivo* coronary plaque morphology assessment: a validation study of *in vivo* virtual histology compared with *in vitro* histopathology. Journal of the American College of Cardiology 2006; 47: 12.

20. Fujii K, Carlier SG, Mintz GS, Wijns W. Association of plaque characterization by intravascular ultrasound virtual histology and arterial remodeling. The American Journal of Cardiology 2005; 96: 1476 –1483.

21. Rodriguez-Granillo GA, García-García HM, McFadden EP. *In vivo* intravascular ultrasound-derived thin-cap fibroatheroma detection using ultrasound radiofrequency data analysis. Journal of the American College of Cardiology 2005; 46: 11.

22. Haralick R, Shanmugam K, Dinstein I. Textural freatures of image classification. IEEE Trans Syst Man Cyber 1973; 6: 610–621.

23. Ojala T, PietikaÈinen M, MaÈenpa T. Multiresolution gray-scale and rotation invariant texture classification with local binary patterns. IEEE Transactions on Pattern Analysis and Machine Intelligence 2002; 24: 7.

24. X. Tang. Texture information in run-length matrices. IEEE Transactions on Image Processing. 1998; 7: 1602-1609.